

## OPTIMIZATION OF THE DESIGNS OF SMALL-SIZE HELIUM CRYOSTATS

N. I. Narykin

UDC 536.581.3

*Using a computer program that simulates thermophysical processes occurring in small helium cryostats, the surface emissivities of actual cryostats are verified. The efficiency of the heat transfer from the walls of the reservoir suspension tube to the helium vapors is determined. The program makes it possible to optimize the designs of cryostats according to the specific conditions of their use.*

High-sensitivity radiation detectors cooled to cryogenic temperatures are used in infrared spectroscopy, astronomy, and other fields of technology. The detectors and the elements of the matching optics and of the electronic circuit are located in small (with a reservoir volume of up to 3 liters) helium cryostats. Most often, cryostats with a single radiation shield cooled by only the evaporating helium vapors (Fig. 1a) or liquid nitrogen are used (Fig. 1b). Sometimes shields are added.

The efficiency of cryostats is increased by optimizing their design for minimal helium evaporation [1-3]. Calculations are performed by computer. However, the absence of reliable data on the characteristics of structural materials and the heat exchange of the walls of the helium reservoir suspension tube with helium vapors makes the practical use of calculations difficult. These factors, as well as the need for a comprehensive approach to creating receiving devices with cooled radiation detectors have stimulated the computer simulation of helium cryostats and the creation of the computer simulation-based methods for seeking optimum design solutions.

In simulation, the helium reservoir suspension tube was considered, as in [2, 3], as a heat exchanger with three zones connected in series (see Fig. 1): 1) a  $L_1$ -long zone of the helium reservoir tube up to the radiation shield holder; 2) a  $L_2$ -long zone of the tube enclosed in the shield holder; 3) a  $L_3$ -long zone of the tube from the radiation shield holder to the upper flange of the cryostat. The heat supplied to the cold parts of the cryostat by radiation and heat conduction as well as that removed by helium and nitrogen vapors were taken into account.

Heat is supplied to the radiation shield by:

- Radiation from the external background through the entrance window of the cryostat,  $q_1$ :

$$q_1 = \sigma \epsilon_{bg} (T_{bg}^4 - T_{sh}^4) \left[ \epsilon_{re1} F_1 + \epsilon_1 F_2 \frac{\Omega_1}{\pi} \right] \tau_1, \tag{1}$$

where

$$\epsilon_{re1} = \frac{\epsilon_{ho} \epsilon_{sh}}{\epsilon_{ho} + \epsilon_{sh} (1 - \epsilon_{ho}) F_{sh}/F_{ho}}; \tag{2}$$

- Radiation from the inner surfaces of the cryostat housing  $q_2$ :

$$q_2 = \sigma (T_{ho}^4 - T_{sh}^4) \left[ \epsilon_{re1} F_{sh} + \epsilon_1 F_2 \left( \epsilon_{re2} + \epsilon_2 \frac{\Omega_1}{\pi} \right) \right], \tag{3}$$

where

---

All-Russian Scientific Center "S. I. Vavilov State Optical Institute," St. Petersburg, Russia. Translated from *Inzhenerno-Fizicheskii Zhurnal*, Vol. 68, No. 5, pp. 760-766, September-October, 1995. Original article submitted March 9, 1993.

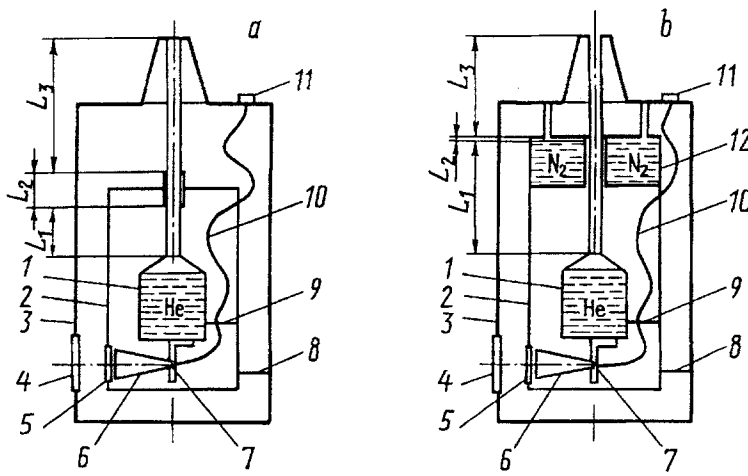


Fig. 1. Schematic diagram of cryostats with one radiation shield: 1) helium reservoir; 2) radiation shield; 3) cryostat housing; 4) entrance window; 5) optical filter; 6) matching optics; 7) radiation detector; 8) mechanical couplings between the housing and shield; 9) mechanical couplings between the shield and helium reservoir; 10) electric wires; 11) electric vacuum joint; 12) nitrogen reservoir.

$$\epsilon_{re2} = \frac{\epsilon_{sh}\epsilon_{ho}}{\epsilon_{sh} + \epsilon_{ho}(1 - \epsilon_{sh})F_{ho}/F_{sh}}; \quad (4)$$

- Heat conduction in the third zone of the tube  $q_3$ :

$$q_3 = \frac{S}{L_3} \int_{T_{sh}}^{T_{ho}} \lambda(T) dT; \quad (5)$$

- Heat conduction of the mechanical couplings that center the shield relative to the housing,  $q_4$ :

$$q_4 = n_1 \frac{S_1}{l_1} \int_{T_{sh}}^{T_{ho}} \lambda_1(T) dT; \quad (6)$$

- Heat conduction along the electric wires over the portion from the joint on the cryostat housing to the radiation shield,  $q_5$ :

$$q_5 = n_2 \frac{S_2}{l_2} \int_{T_{sh}}^{T_{ho}} \lambda_2(T) dT; \quad (7)$$

- Heating of the wires over this portion by the electric current passing through them,  $q_6$ :

$$q_6 = n_2 \rho \frac{l_2}{S_2} I^2. \quad (8)$$

The total heat supply to the radiation shield  $q_{sh}^+$  is:

$$q_{sh}^+ = \sum_{i=1}^6 q_i. \quad (9)$$

Heat is removed from the radiation shield by:

- Radiation from its inner surfaces,  $q_7$ :

$$q_7 = \sigma (T_{\text{sh}}^4 - T_{\text{res}}^4) [\varepsilon_{\text{re}_3} F_{\text{res}} + \varepsilon_1 \varepsilon_{\text{res}} F_2], \quad (10)$$

where

$$\varepsilon_{\text{re}_3} = \frac{\varepsilon_{\text{sh}} \varepsilon_{\text{res}}}{\varepsilon_{\text{sh}} + \varepsilon_{\text{res}} (1 - \varepsilon_{\text{sh}}) F_{\text{res}} / F_{\text{sh}}}; \quad (11)$$

- Heat conduction in the first zone of the tube,  $q_8$ :

$$q_8 = \frac{S}{L_1} \int_{T_{\text{res}}}^{T_{\text{sh}}} \lambda(T) dT; \quad (12)$$

- Heat conduction of the mechanical couplings that center the reservoir relative to the shield,  $q_9$ :

$$q_9 = n_3 \frac{S_3}{l_3} \int_{T_{\text{res}}}^{T_{\text{sh}}} \lambda_3(T) dT; \quad (13)$$

- Heat conduction along the electric wires over the portion from the shield to the helium reservoir,  $q_{10}$ :

$$q_{10} = n_2 \frac{S_2}{l_4} \int_{T_{\text{res}}}^{T_{\text{sh}}} \lambda_2(T) dT; \quad (14)$$

- Evaporation of liquid nitrogen and removal of heat by helium vapors from the walls of the tube in the second and third zones,  $q_{11}$ :

$$q_{11} = G_1 r_1 + \pi d (L_2' U_2 \Delta T_2 + L_3' U_3 \Delta T_3). \quad (15)$$

The total heat removal from the radiation shield  $q_{\text{sh}}^-$  is:

$$q_{\text{sh}}^- = \sum_{i=7}^{10} q_i + G_1 r_1 + \pi d (L_2' U_2 \Delta T_2 + L_3' U_3 \Delta T_3). \quad (16)$$

$$q_{\text{sh}}^+ = q_{\text{sh}}^-. \quad (17)$$

Heat to the reservoir with liquid helium is supplied by:

- Radiation and heat conduction from the radiation shield,  $q_{12}$ :

$$q_{12} = \sum_{i=7}^{10} q_i; \quad (18)$$

- Radiation from the external background through the inlet window to the cryostat housing and the optical filter on the radiation shield,  $q_{13}$ :

$$q_{13} = \sigma \varepsilon_{\text{bg}} \varepsilon_{\text{det}} F_3 (T_{\text{bg}}^4 - T_{\text{res}}^4) \frac{\Omega_2}{\pi} \tau_1 \tau_2 \tau_3; \quad (19)$$

- Radiation from the inner surfaces of the cryostat housing,  $q_{14}$ :

$$q_{14} = \sigma (T_{\text{ho}}^4 - T_{\text{res}}^4) \left[ \varepsilon_{\text{re}_2} \varepsilon_{\text{re}_3} (F_2 - F_3) \frac{\pi - \Omega_2}{\pi} + \varepsilon_2 \varepsilon_{\text{det}} F_3 \frac{\Omega_2}{\pi} \tau_3 \right] \tau_2; \quad (20)$$

- Heating of the wires over the portion from the shield to the helium reservoir and by the electric power  $P$  liberated in the radiation detector and elements of its electric circuit,  $q_{15}$ :

$$q_{15} = n_{\mathcal{P}} \frac{l_4}{S_2} I^2 + p. \quad (21)$$

Heat from the reservoir with liquid helium is removed by:

- Evaporation of liquid helium and removal of heat by its vapors from the tube walls in the first zone,  $q_{16}$ :

$$q_{16} = Gr + \pi d L_1' U_1 \Delta T_1. \quad (22)$$

The heat balance equation for the reservoir with liquid helium is:

$$\sum_{i=7}^{10} q_i + \sum_{i=13}^{15} q_i = Gr + \pi d L_1' U_1 \Delta T_1. \quad (23)$$

With account for (16) and (17) and after substitutions, Eq. (23) takes the following form:

$$q_{sh}^+ + q_{det} = \pi d \sum_{k=1}^3 L_k' U_k \Delta T_k + G_1 r_1 + Gr, \quad (24)$$

where

$$q_{det} = \sum_{i=13}^{15} q_i. \quad (25)$$

The heat  $q_{det}$  determined by the operating conditions of the radiation detector is an inseparable part of heat supply to the helium reservoir. Therefore, in conformity with Eq. (24), the efficiency of the use of the heat content of liquid helium  $E$  in the cryostat is

$$E = q_{det} / \left[ q_{det} + \left( q_{sh}^+ - \pi d \sum_{k=1}^3 L_k' U_k \Delta T_k - G_1 r_1 \right) \right]. \quad (26)$$

We should note that the system of equations (1)-(26) describes the thermophysical processes occurring in both cryostats with and without cooling a radiation shield by liquid nitrogen. In the latter case, simply  $G_1 = 0$ . Ultimately, simulation is reduced to finding values for the thermal parameters of the cryostat at which heat balance is attained simultaneously on the radiation shield and on the helium reservoir.

A computer program was developed which, after collection of the initial data concerning the design elements of the cryostat, its type, and helium temperature, finds the values of  $L_k'$  and  $T_{sh}$  corresponding to the minimum value of helium evaporability  $G$ . Using these data, as well as operating with the efficiency of the use of the liquid-helium heat content  $E$ , it is possible to correct the design. Other conditions being equal, the cryostat has minimal dimensions and mass when the lengths of the tube portions  $L_k'$  participating in heat exchange with helium vapors are equal to the lengths  $L_k$  of the corresponding zones. Zone lengths  $L_k$  greater than  $L_k'$  do not lead to a decrease in the evaporability of helium, while smaller ones cause its increase.

The program was verified by simulating an experiment with a nitrogen-free helium cryostat (with a reservoir capacity equal to 0.5 liter); information on this can be found in [3] for a study of the influence exerted by the zone lengths  $L_k$  of a 1X18H9T stainless-steel tube with outer diameter 12 mm and wall thickness 0.2 mm on the helium evaporability  $G$  and the radiation-shield temperature  $T_{sh}$ . The surface areas of the housing  $F_{ho}$ , shield  $F_{sh}$ , and reservoir  $F_{res}$  of the cryostat were equal to  $9.6 \cdot 10^{-2} \text{ m}^2$ ,  $6.3 \cdot 10^{-2} \text{ m}^2$ , and  $3.6 \cdot 10^{-2} \text{ m}^2$ , respectively. According to calculations that assume a laminar helium-vapor flow in the tube, the optimum lengths of the tube zones should be  $L_1 = 46 \text{ mm}$ ,  $L_2 = 22 \text{ mm}$ , and  $L_3 = 27 \text{ mm}$ . When investigating one of the zones of the tube, the other two had the design dimensions. The primary length of the tube was taken to be larger than that predicted by 15–20 mm. After successive measurements of the values of  $G$  and  $T_{sh}$ , the tube length was altered

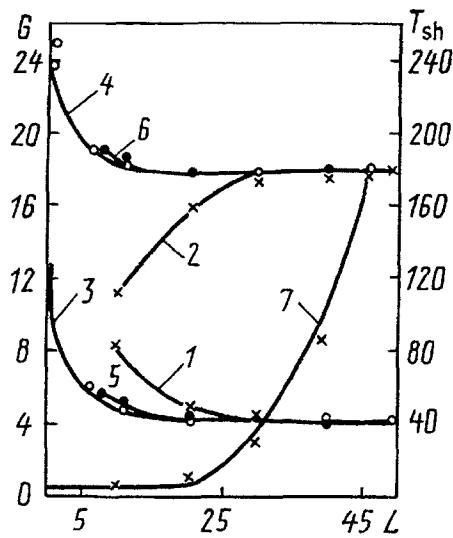


Fig. 2. Dependences of the rates of helium evaporation (gr/h) and radiation shield temperature (K) on the tube length (mm) of a 0.5-liter nitrogen-free cryostat in the first (1 and 2), second (3 and 4), and third zone (5 and 6); temperature profile of the tube in the first zone (7).

by cutting and subsequent resoldering. Everything seems to indicate that the auxiliary shield was removed from the helium reservoir for this reason. As a result, the area  $F_{res}$  was equal not to  $4.7 \cdot 10^{-2} \text{ m}^2$ , as it was initially in [2], but was diminished by the magnitude of the side surface area of this shield and was equal to  $3.6 \cdot 10^{-2} \text{ m}^2$ . This is also proved by the fact that for the same helium evaporability the temperature of the radiation shield in [2] was lower by 12 K and amounted to 166 K.

While verifying the program, the length of one of the zones of the tube was altered and the design lengths of the other two were preserved. In this case, the emissivities  $\epsilon_{ho}$ ,  $\epsilon_{sh}$  and  $\epsilon_{res}$  were varied, as well as the mathematical expressions and parameters in them that determine the magnitudes of heat fluxes exchanged between the walls of the tube zones and the evaporated helium flow. The criterion was the maximum approximation of the calculated values of  $G$  and  $T_{sh}$  to those obtained in the experiment.

It was found that the best agreement of calculation with experiment was observed when the tube was considered a heat exchanger with a turbulent gas flow in it, when the magnitude of the heat flux  $q_k$  removed from the walls of the tube by helium vapors in the  $k$ -th zone was calculated from the formula given in [4]:

$$q_k = \pi d L_k \frac{U_c \Delta T_w - U_w \Delta T_c}{\ln(U_c \Delta T_w / U_w \Delta T_c)}, \quad (27)$$

the heat conduction coefficients on the "cold"  $U_c$  and "warm"  $U_w$  ends of the zones were calculated from the MacAdams formula, which was transformed by taking into account the temperature dependences of the thermal conductivity and viscosity of the vapor:

$$U = m \cdot 0.84 \frac{1}{d} \left( \frac{G}{d} \right)^{0.8} T_h^{0.12} \text{ kcal}/(\text{m}^2 \cdot \text{h} \cdot \text{K}), \quad (28)$$

in which the dimensionless coefficient  $m$  was used to take into account the change in the heat transfer of the tube walls in transition from one zone to the other.

The helium-vapor temperature  $T_h$  at the inlet to the tube was assumed equal to the liquid helium temperature, while on the "warm" end of the  $k$ -th zone and correspondingly on the "cold" end of the subsequent zone it was determined from the equation:

$$G c_p (T_w - T_c) = q_k. \quad (29)$$

The temperature difference  $\Delta T$  of the helium vapors at the inlet to the tube was calculated from the formula

$$\Delta T = 1.1 \cdot 10^{-5} + 6.42 \cdot 10^9 (\Delta G)^{4.7} \quad [K], \quad (30)$$

while on the "warm" end of the  $k$ -th zone and correspondingly on the "cold" end of the subsequent zone it was determined as the difference between the temperatures of the radiation shield or cryostat housing and the helium vapors.

The dependences of the rates of helium evaporation and radiation shield temperature on the length of the tube zones and the temperature profile in the first zone of the tube of this cryostat are presented in Fig. 2. Calculations were performed at the following values of the parameters: the emissivities of the reservoir surfaces, shield, and cryostat housing were 0.0132, 0.0688, and 0.0689, respectively; the heat-transfer coefficients of the tube walls of the 1st, 2nd, and 3rd zones were 0.80, 0.44, and 0.80. For comparison, the figure contains experimental values of [3]. Analysis of the calculation results made shows their agreement with the experiment within the errors of measurements. This makes it possible to conclude that the program developed rather accurately simulates the thermophysical processes occurring in a cryostat and, consequently, can be used to optimize the designs of cryostats.

## NOTATION

$\sigma$ , Stefan-Boltzmann, constant;  $\epsilon_{bg}$ ,  $\epsilon_{ho}$ ,  $\epsilon_{sh}$ ,  $\epsilon_{res}$ ,  $\epsilon_{det}$ , emissivities of the background surrounding the cryostat, housing surface of the cryostat, radiation shield, helium reservoir, and radiation detector;  $T_{bg}$ ,  $T_{ho}$ ,  $T_{sh}$ ,  $T_{res}$ , temperatures of the background, cryostat housing, shield, and reservoir;  $\epsilon_{re1}$ ,  $\epsilon_{re2}$ ,  $\epsilon_{re3}$ , reduced emissivities of the shield, housing, and reservoir;  $F_{sh}$ ,  $F_{ho}$ ,  $F_{res}$ , surface areas of shield, housing, and reservoir;  $F_1$ ,  $F_2$ ,  $F_3$ , areas of the entrance window in the cryostat housing, of the filter on the radiation shield, and of the inlet hole of the matching optics;  $\epsilon_1$ ,  $\epsilon_2$ , emissivities of the filter and entrance window;  $\Omega_1$ , solid angle at which the background radiation is absorbed by optical filter;  $\Omega_2$ , solid angle at which radiation is transferred by matching optics to the radiation detector;  $\tau_1$ ,  $\tau_2$ ,  $\tau_3$ , transmission of radiation by way of the entrance window, filter, and matching optics;  $S$ , cross-sectional area of the helium reservoir suspension tube;  $\lambda(T)$ , temperature dependence of the thermal conductivity of the tube material;  $n_1$ ,  $n_2$ ,  $n_3$ , number of mechanical couplings between the housing and the shield, electric wires, and mechanical couplings between the shield and reservoir;  $S_1$ ,  $S_2$ ,  $S_3$ , cross-sectional areas of the mechanical coupling between the housing and shield, of the electric wire, and of the mechanical coupling between the shield and reservoir;  $l_1$ ,  $l_2$ ,  $l_3$ ,  $l_4$ , lengths of mechanical couplings and electric wires over the body-shield and the shield-reservoir portions;  $\lambda_1(T)$ ,  $\lambda_2(T)$ ,  $\lambda_3(T)$ , temperature dependences of the thermal conductivities of the materials of mechanical couplings between the housing and shield, of electric wires, and mechanical couplings between the shield and reservoir;  $\rho$ , specific resistance of the material of electric wires;  $I$ , working electric current;  $d$ , inner diameter of the helium reservoir suspension tube;  $L_1$ ,  $L_2$ ,  $L_3$ , lengths of the portions of the tube in the first, second, and third zones participating in heat exchange with helium vapors;  $U_1$ ,  $U_2$ ,  $U_3$ , coefficients of heat conduction from the tube walls to helium vapors in the first, second, and third zones;  $\Delta T_1$ ,  $\Delta T_2$ ,  $\Delta T_3$ , temperature differences in the corresponding zones of the tube;  $G_1$ , weighted quantity of nitrogen evaporated per unit time;  $r_1$ , latent heat of nitrogen vapor generation;  $G$ , weighted quantity of helium evaporated per unit time;  $r$ , latent heat of helium vapor generation;  $T_h$ , temperature of helium vapors;  $c_p$ , heat capacity of gaseous helium;  $\Delta G$ , weighted quantity of helium evaporated per unit time due to heat supply only along the helium reservoir suspension tube.

## REFERENCES

1. C. Ceccarelli, G. D. Oglio, M. D. Bari, L. Pizzo, and C. Santillo, *Cryogenics*, **30**, No. 6, 530-532 (1990).
2. V. S. Golubkov and N. A. Pankratov, *Inzh.-Fiz. Zh.*, **19**, No. 1, 52-61 (1970).
3. V. S. Golubkov and N. A. Pankratov, *Inzh.-Fiz. Zh.*, **26**, No. 2, 220-225 (1974).
4. R. B. Scott, in: *Low-Temperature Technique* [Russian translation], Moscow (1962), pp. 26-38.